



## ATLAS NOTE

ATLAS-PHYS-PUB-2012-005

November 28, 2012



# Studies of Vector Boson Scattering with an Upgraded ATLAS Detector at a High-Luminosity LHC

The ATLAS Collaboration

### Abstract

The Phase 2 upgrade of the ATLAS detector would greatly increase the sensitivity to an extended electroweak symmetry-breaking sector beyond the Standard Model Higgs mechanism. A common feature of such an extended sector is the enhancement of longitudinal vector boson scattering at high energy. Using simplified detector performance parameterizations, we present the expected gain in sensitivity if the ATLAS dataset were increased from  $300 \text{ fb}^{-1}$  to  $1 \text{ ab}^{-1}$  and  $3 \text{ ab}^{-1}$  at a center-of-mass energy of 14 TeV.

## 1 Introduction

The exploration of physics at the TeV scale is the major goal of the LHC, and the luminosity upgrade of the LHC can have a major impact in discovering an extended electroweak symmetry-breaking sector beyond the Standard Model (SM) Higgs mechanism.

A major reason for expecting new particles or interactions at the TeV energy scale has been the prediction that an untamed rise of the vector boson scattering (VBS) cross section in the longitudinal mode would violate unitarity at this scale. In the SM it is the Higgs particle which is responsible for the damping of this cross section. It is important to confirm this effect experimentally. Alternate models such as Technicolor and little Higgs have been postulated which encompass TeV-scale resonances and a light scalar particle. Other mechanisms for enhancing vector boson scattering at high energy are possible, even after the existence of the SM Higgs boson is established.

A striking experimental feature of vector boson scattering is the presence of two high- $p_T$  jets in the forward-backward regions, similar to those found in Higgs production via vector boson fusion. The absence of color exchange in the hard scattering process leads to rapidity gaps in the central part of the detector; however the gap topology will be difficult to exploit due to the high level of pileup at a high-luminosity LHC.

We present studies of sensitivity to beyond-SM (BSM) scenarios for three final states:  $WW$  in the lepton plus jets channel,  $WW$  in the dilepton channel, and  $ZZ$  in the 4-lepton channel. Both  $WW$  analyses were included in the initial Cracow submission [1], while the  $ZZ$  study is included here as an update to that document.

## 2 Theoretical Descriptions of $VV$ Scattering

At next-to-leading order, the generalized electroweak chiral Lagrangian (EWChL) contains eleven bosonic terms that are  $C$ - and  $CP$ -invariant. Of these, three terms induce oblique corrections to the gauge boson propagators, and another three terms contribute to anomalous trilinear gauge couplings. The remaining five operators induce anomalous quartic couplings only, of which two conserve weak isospin (i.e. maintain the custodial  $SU(2)$  symmetry) to all orders as suggested by  $\Delta\rho = (\rho - 1) \approx 0$ , where  $\rho = m_W^2/m_Z^2 \cos^2 \theta_W$ . These two operators are scaled by the numerical coefficients  $a_4$  and  $a_5$ . In the following, we have investigated two separate approaches to unitarizing the scattering amplitudes from the EWChL. The first approach is based on the Padé unitarization (or Inverse Amplitude Method) in the model of Dobado et al. [2], which allows for a single new physics resonance that unitarizes the scattering amplitude. With this method, the resonance mass, width, and couplings are fully determined by the coefficients  $a_4$  and  $a_5$ . The second approach is based on a scheme that includes high-mass resonances with the low-energy behavior of the EWChL, using a minimal K-matrix unitarization method [3].

## 3 Monte Carlo Simulation

SM and BSM predictions were generated using Monte Carlo (MC) techniques. Events were simulated using several MC generators (see analysis-specific details below). Particle showers were simulated using Pythia version 8.1 [4]. Outgoing truth-level electrons, photons, and hadrons were clustered into anti- $k_T$  jets with  $R = 0.4$  unless otherwise noted.

The sensitivity to new physics in vector boson scattering depends on jet, lepton and missing energy reconstruction in the high-pileup regime. Fully simulated events under high-pileup conditions have been produced, and efficiencies and resolutions have been estimated for the various objects by the combined performance groups. These quantities have been used to smear particle-level outputs for various new-physics scenarios [5].

## 4 Object Selection

As mentioned previously, final state particles were taken from the truth-level Monte Carlo output, and their four-momenta were smeared according to pileup-dependent parameterizations. The smeared quantities are used in the event selection. Reconstruction and trigger efficiencies are also parametrized in fully simulated events [5].

Objects are required to pass these selection criteria in all analyses below, unless otherwise noted.

- Electrons:  $E_T > 25$  GeV,  $|\eta| < 2.47$  (excluding  $1.37 < |\eta| < 1.52$ )
- Muons:  $p_T > 25$  GeV,  $|\eta| < 2.4$
- Jets:  $p_T > 50$  GeV,  $|\eta| < 4.9$

In order to avoid reconstructing electrons as jets, the nearest jet to a selected electron is removed, provided the separation between them satisfies  $\Delta R = \sqrt{(\Delta\eta)^2 + (\Delta\phi)^2} < 0.2$ . Any electron within  $\Delta R < 0.2$  of a selected jet after this overlap removal is also removed.

The missing transverse energy ( $E_T^{\text{miss}}$ ) of an event is defined as the negative vector sum of the transverse momenta of true stable interacting particles, smeared with the appropriate resolution.

## 5 WW in the Lepton Plus Jets Channel

This analysis was included in the ATLAS submission to the Cracow symposium on the European Strategy for Particle Physics [1].

### 5.1 Introduction

The  $WW$  mass spectrum at high mass is sensitive to BSM diboson resonances. One advantage of the lepton plus jets channel is the ability to fully reconstruct each  $W$  boson four-momentum and calculate the  $WW$  invariant mass. In this analysis, forward and backward jets are used to tag VBS events, and the reconstructed lepton,  $E_T^{\text{miss}}$ , and hadronic  $W$  are combined to determine the  $WW$  invariant mass.

### 5.2 Event Selection

Events are considered VBS  $WW$  lepton plus jets candidates provided they meet the following criteria:

- One lepton with  $p_T > 60$  GeV
- $E_T^{\text{miss}} > 25$  GeV
- The combined lepton- $E_T^{\text{miss}}$  system must have  $p_T > 200$  GeV.
- Two anti- $k_t$   $R = 0.4$  jets with  $p_T > 40$  GeV which are in opposing  $\eta$  hemispheres and separated by at least  $\Delta\eta > 5$  (tag jets)
- One tag jet with  $E > 500$  GeV and the second with  $E > 300$  GeV
- $m_{jj} > 250$  GeV, where  $m_{jj}$  is the invariant mass of the two tag jets
- One anti- $k_t$   $R = 0.6$  jet with  $p_T > 300$  GeV and  $60 \text{ GeV} < m < 110 \text{ GeV}$  ( $W$ -jet)

The  $p_z$  of the neutrino is determined by imposing the  $W$  boson mass constraint on the lepton-neutrino system. The reconstructed  $WW$  invariant mass ( $m_{WW}$ ) is the mass formed by the sum of the neutrino, lepton, and  $W$ -jet four-momenta.

In order to reject  $t\bar{t}$  events, a top quark veto is applied. The four-momentum of each anti- $k_t$   $R = 0.4$  jet with  $p_T > 40$  GeV is combined with that of the  $W$ -jet, and if any combination has a mass  $140 \text{ GeV} < m < 240 \text{ GeV}$  the event is discarded.

### 5.3 Statistical Analysis

The background is dominated by  $t\bar{t}$  and diboson events. The  $W + 3$  jets and  $W + 4$  jets backgrounds are not significant. The dominant backgrounds are compared to resonance hypotheses obtained from the generalized chiral Lagrangian model; the predicted width of  $\mathcal{O}(100 \text{ GeV})$  is determined by the  $(a_4, a_5)$  values given in the table.

Quoted in Table 1 is the significance of the resonant excess over background for integrated luminosity of  $300 \text{ fb}^{-1}$  and  $3000 \text{ fb}^{-1}$ . These numbers illustrate the discovery potential for a new vector resonance of mass  $\sim 1 \text{ TeV}$ , which is an interesting mass range to probe in the context of electroweak symmetry-breaking. The increase by a factor of ten in integrated luminosity enables these searches to cross the discovery threshold. These predictions are conservative; better sensitivity is expected with an improved top-quark veto using  $b$ -tagged central jets.

model ( $a_4, a_5$ )	SM (0, 0)	500 GeV scalar (0.01, 0.009)	800 GeV vector (0.009, -0.007)	1150 GeV vector (0.004, -0.004)
$S/B$	$(3.3 \pm 0.3)\%$	$(0.7 \pm 0.1)\%$	$(4.9 \pm 0.3)\%$	$(5.8 \pm 0.3)\%$
$S/\sqrt{B} (L = 300 \text{ fb}^{-1})$	$2.3 \pm 0.3$	$0.6 \pm 0.1$	$3.3 \pm 0.4$	$3.9 \pm 0.4$
$S/\sqrt{B} (L = 3000 \text{ fb}^{-1})$	$7.2 \pm 0.1$	$1.6 \pm 0.1$	$10.4 \pm 0.7$	$12.4 \pm 0.7$

Table 1: Summary of sensitivity to various resonance hypotheses in the  $WW$  lepton plus jets channel. Monte Carlo statistical uncertainties on the sensitivity estimates are also shown.

## 6 $WW$ in the Dilepton Final State

This analysis was included in the Cracow submission [1].

### 6.1 Introduction

The  $WW$  scattering cross section at high diboson mass is sensitive to  $a_4$  and  $a_5$ . In this analysis  $a_5$  is set to zero and the sensitivity to  $a_4$  is studied.

The two leading jets are used to tag the diboson fusion process  $pp \rightarrow WW + 2j \rightarrow e\nu\mu\nu + 2j$ . The dilepton channel is relatively free of mis-identification backgrounds from  $W$ -jets and QCD multi-jet processes, and the  $e\mu$  channel is also free from the  $Z$ -jets background. We protect against jet mis-identification backgrounds by requiring the tagging jets to have  $p_T > 50$  GeV. The dominant background is from  $t\bar{t}$  production, followed by diboson production.

### 6.2 Monte Carlo Predictions

Pythia8 was used to generate the SM  $t\bar{t}$  and SM non-VBS  $WW$  backgrounds. Pythia6 with an EWChL extension was used to generate  $WW$  scattering events for various values of  $a_4$  (including  $a_4 = 0$ ). Table 2 enumerates the cross sections of various processes in the dilepton channel at  $\sqrt{s} = 14 \text{ TeV}$ .

Process	$\sigma$ BR (fb)
$t\bar{t}$	$43.0 \times 10^3$
$a_4 = 0$	2.21
$a_4 = 0.003$	3.33
$a_4 = 0.01$	7.11
$a_4 = 0.03$	18.7

Table 2: Summary of  $WW$  production cross sections at  $\sqrt{s} = 14$  GeV, with  $a_5 = 0$ .

model	$300 \text{ fb}^{-1}$	$1 \text{ ab}^{-1}$	$3 \text{ ab}^{-1}$
$a_4$	0.066	0.025	0.016

Table 3: Summary of expected upper limits for  $a_4$  at the 95% confidence level using the  $pp \rightarrow WW + 2j \rightarrow e\mu + 2j$  search at  $pp$  collision center-of-mass energy of 14 TeV.

### 6.3 Event Selection

Events are considered VBS  $WW$  candidates provided they meet the following criteria:

- Exactly one selected muon and one selected electron with opposite charges
- At least one selected lepton must fire the trigger.
- At least two selected jets
- At least 50 GeV of  $E_T^{\text{miss}}$

### 6.4 Statistical Analysis

The statistical analysis is performed by constructing templates of the  $m_{lljj}$  distribution for backgrounds plus  $WW$  signal at different values of  $a_4$ . Here  $m_{lljj}$  is the 4-body invariant mass of the two leading leptons and the two leading jets in the event, which we found to be a robust and sensitive variable since calculating the true  $WW$  invariant mass is not possible when two neutrinos are present. At each value of  $a_4$ , the likelihood function of the floated signal cross section is defined as the Poisson probability product over all  $m_{lljj}$  bins for the pseudo-data given the expectation in each bin. The diboson background normalization is given by the theory cross section, while the  $t\bar{t}$  background is floated and is effectively constrained by the low- $m_{lljj}$  region. The  $WW$  scattering background in the absence of new physics is included in this analysis by considering the case  $a_4 = 0$ . The expected upper limits on  $a_4$ , which we quote as a measure of sensitivity, are shown in Table 1. The distribution of  $m_{lljj}$  and a representative limit curve as a function of  $a_4$  are shown in Figure 1.

## 7 ZZ in the Four Lepton Final State

This analysis is new since the Cracow submission [1].

### 7.1 Introduction

The fully leptonic  $ZZjj \rightarrow \ell\ell\ell\ell jj$  channel has a small cross section but provides a clean, fully reconstructible  $ZZ$  resonance peak. A forward jet-jet mass requirement of 1 TeV reduces the contribution from jets accompanying non-VBS diboson production. Figure 2 shows the jet-jet invariant mass distribution

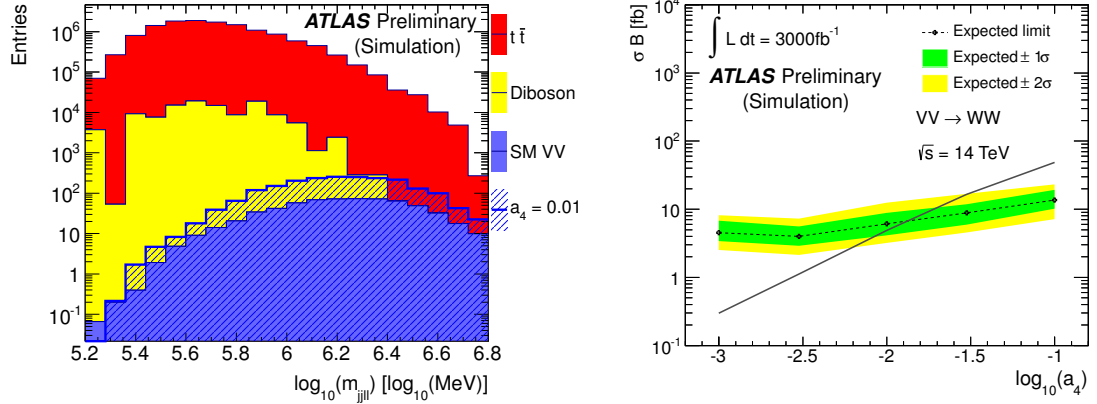


Figure 1: The reconstructed 4-body mass spectrum using the two leading leptons and jets (left) and limits as a function of  $a_4$  using the  $e\mu$  channel with  $3 \text{ ab}^{-1}$  at  $pp$  center-of-mass collision energy of 14 TeV. The background labelled “SM VV” corresponds to  $a_4 = 0$ .

and the reconstructed 4-lepton invariant mass distribution. The high-mass resonance is easily visible in this simulated dataset normalized to  $3000 \text{ fb}^{-1}$ .

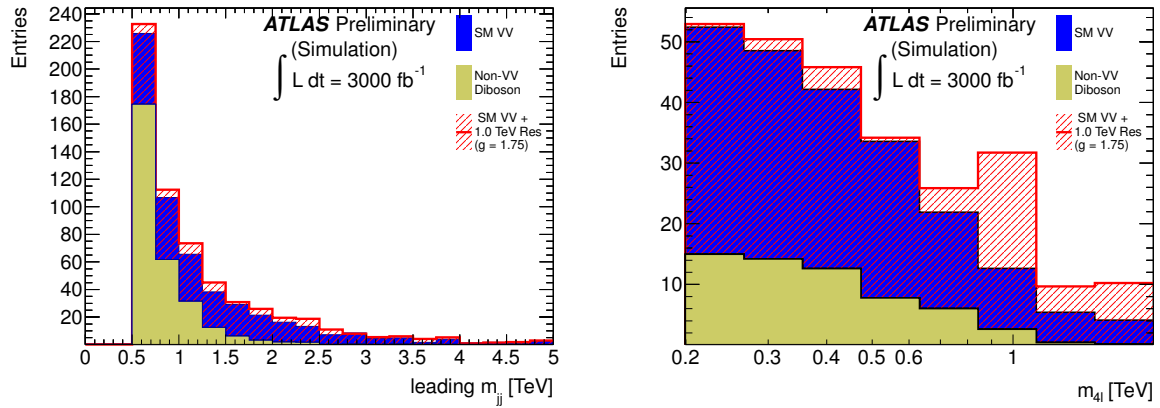


Figure 2: The leading jet-jet invariant mass ( $m_{jj}$ ) distribution for simulated events in the  $pp \rightarrow ZZ + 2j \rightarrow \ell\ell\ell\ell + 2j$  channel (left), and the reconstructed 4-lepton mass ( $m_{4\ell}$ ) spectrum for this channel after requiring  $m_{jj} > 1 \text{ TeV}$  (right). The spectra are normalized to  $3000 \text{ fb}^{-1}$ .

## 7.2 Monte Carlo Predictions

MadGraph 1.4.2 [6] was used to generate the non-VBS background where  $ZZ$  production is accompanied by initial-state radiation of two jets. SM and non-SM  $ZZ$  production via VBS was simulated using WHIZARD 2.1.0 [7]. In both cases  $Z$  bosons were required to decay to electron or muon pairs. Table 4 enumerates the cross sections of various processes in the four-lepton channel at  $\sqrt{s} = 14 \text{ TeV}$ .

## 7.3 Event Selection

Events are considered VBS  $ZZ$  candidates provided they meet the following criteria:

- Exactly four selected leptons which can be separated into two opposite sign, same flavor pairs

Process	$\sigma$ BR (fb)
non-VBS $ZZjj$	6.66
SM VBS $ZZ$	0.80
SM VBS + 500 GeV Resonance, $g = 1.0$	1.03
SM VBS + 1 TeV Resonance, $g = 1.75$	0.91
SM VBS + 1 TeV Resonance, $g = 2.5$	0.98

Table 4: Summary of  $ZZ \rightarrow 4\ell$  production cross sections. The non-VBS  $ZZjj$  background was generated with a jet  $p_T > 20$  GeV requirement.

- At least one selected lepton must fire the trigger.
- At least two selected jets
- $m_{jj} > 1$  TeV, where  $m_{jj}$  is the invariant mass of the two highest- $p_T$  selected jets

#### 7.4 Statistical Analysis

In order to determine the expected sensitivity to BSM  $ZZ$  resonances, the background-only  $p_0$ -value expected for signal+background is calculated using the  $m_{4\ell}$  spectrum. In Table 5 the  $p_0$ -values have been converted to the corresponding number of Gaussian  $\sigma$  in significance. The increase in significance with integrated luminosity is shown for different resonance masses and couplings.

model	$300 \text{ fb}^{-1}$	$3000 \text{ fb}^{-1}$
$m_{\text{resonance}} = 500 \text{ GeV}, g = 1.0$	$2.4\sigma$	$7.5\sigma$
$m_{\text{resonance}} = 1 \text{ TeV}, g = 1.75$	$1.7\sigma$	$5.5\sigma$
$m_{\text{resonance}} = 1 \text{ TeV}, g = 2.5$	$3.0\sigma$	$9.4\sigma$

Table 5: Summary of expected sensitivity to anomalous VBS  $ZZ$  signal at  $\sqrt{s} = 14$  TeV, quoted in the terms of the expected number of Gaussian  $\sigma$  in significance.

In terms of measuring the integrated cross section for the purely-electroweak SM process  $pp \rightarrow ZZ + 2j \rightarrow 4\ell + 2j$ , a statistical precision of 10% is achievable with  $3000 \text{ fb}^{-1}$ , compared to 30% with  $300 \text{ fb}^{-1}$  in the signal-enhanced kinematic region of  $m_{jj} > 1$  TeV and the 4-lepton invariant mass  $m_{4\ell} > 200$  GeV. In the higher mass range of  $m_{4\ell} > 500$  GeV, the corresponding statistical precision achievable would be 15% or 45% with  $3000 \text{ fb}^{-1}$  or  $300 \text{ fb}^{-1}$ , respectively. The larger integrated luminosity is required to enable definitive measurements of the cross section for this important process.

## 8 Conclusions

We have shown results of sensitivity studies for high-mass  $WW$  and  $ZZ$  scattering in an extended Higgs sector, comparing ATLAS datasets of  $300 \text{ fb}^{-1}$ ,  $1 \text{ ab}^{-1}$  and  $3 \text{ ab}^{-1}$  of integrated luminosity at a  $pp$  collision center-of-mass energy of 14 TeV. We have used the  $a_4$  parameter in the generalized electroweak chiral Lagrangian and the mass and couplings of  $VV$  resonances as benchmark parameters. The increase of a factor of ten in integrated luminosity makes ATLAS sensitive to potential high-mass BSM  $VV$  resonances and  $a_4$  values smaller by a factor of four.

For a range of parameter values in models of new physics, new resonances in weak boson scattering in the  $ZZ \rightarrow 4\ell$  final state can only be discovered with the increased integrated luminosity. The increased integrated luminosity is also needed to make a definitive measurement of the SM cross section and to

test if the unitarization of the high-energy  $VV$ -scattering amplitudes is occurring as predicted by the SM Higgs mechanism.

## References

- [1] ATLAS Collaboration, *Physics at a High-Luminosity LHC with ATLAS*, Tech. Rep. ATL-PHYS-PUB-2012-001, CERN, Geneva, Aug, 2012.
- [2] A. Dobado, M. Herrero, J. Pelaez, and E. Ruiz Morales, *CERN LHC sensitivity to the resonance spectrum of a minimal strongly interacting electroweak symmetry breaking sector*, Phys. Rev. **D62** (2000) 055011, [arXiv:hep-ph/9912224](https://arxiv.org/abs/hep-ph/9912224) [hep-ph]. (and references therein).
- [3] A. Alboteanu, W. Kilian, and J. Reuter, *Resonances and Unitarity in Weak Boson Scattering at the LHC*, JHEP **0811** (2008) 010, [arXiv:0806.4145](https://arxiv.org/abs/0806.4145) [hep-ph].
- [4] T. Sjostrand, S. Mrenna, and P. Z. Skands, *A Brief Introduction to PYTHIA 8.1*, Comput.Phys.Commun. **178** (2008) 852–867, [arXiv:0710.3820](https://arxiv.org/abs/0710.3820) [hep-ph].
- [5] ATLAS Collaboration, *Performance inputs to the 2012 European Strategy studies*, Tech. Rep. ATL-COM-UPGRADE-2012-032, CERN, Geneva, 2012.  
<https://cdsweb.cern.ch/record/1483523>.
- [6] J. Alwall, M. Herquet, F. Maltoni, O. Mattelaer, and T. Stelzer, *MadGraph 5 : Going Beyond*, JHEP **1106** (2011) 128, [arXiv:1106.0522](https://arxiv.org/abs/1106.0522) [hep-ph].
- [7] W. Kilian, T. Ohl, and J. Reuter, *WHIZARD: Simulating Multi-Particle Processes at LHC and ILC*, Eur.Phys.J. **C71** (2011) 1742, [arXiv:0708.4233](https://arxiv.org/abs/0708.4233) [hep-ph].